Journal of Magnetic Resonance **148,** 459–464 (2001)
doi:10.1006/jmre.2000.2258, available online at http://www.idealibrary.com on IDEAL®

Fast MAS Total Through-Bond Correlation Spectroscopy[1]

Edme H. Hardy, René Verel, and Beat H. Meier

Laboratory for Physical Chemistry, ETH-Zentrum, 8092 Zurich, Switzerland

E-mail: edha@nmr.phys.chem.ethz.ch; reve@nmr.phys.chem.ethz.ch; beme@nmr.phys.chem.ethz.ch

Received August 14, 2000; revised November 9, 2000

Mixing sequences for total through-bond correlation spectroscopy in solids (TOBSY) were developed. The motivation is the design of broadband, effective, and robust sequences adapted for "fast" MAS. Possible sequences with the desired Hamiltonian (the homonuclear isotropic *J* interaction) were identified using lowest order average Hamiltonian theory. Numerical simulations as a function of the MAS frequency were then employed to further characterize the performance. An experimental TOBSY spectrum of a uniformly ^{13}C-labeled decapeptide at 20 kHz MAS was obtained using one of the new sequences. The spectrum allows us to assign the ^{13}C resonances to the respective spin systems. © 2001 Academic Press

Key Words: **fast MAS; scalar coupling; total correlation spectroscopy; TOBSY; antamanide.**

1. INTRODUCTION

Total correlation spectroscopy (TOCSY) (*1*) is a two-dimensional correlation experiment that leads to cross peaks between all resonance lines of a coupled spin system and is a useful tool for assignment. In the case of overlapping lines, the spectral resolution can be drastically enhanced compared to the one-dimensional spectrum. TOCSY is particularly useful in peptides and proteins where, to good approximation, each residue is described by an independent spin system (*2*). TOCSY was first and is still frequently applied to solutions. There the coupling interaction is the scalar *J* coupling. In solids, either the scalar or the dipolar coupling may be used. To distinguish between the two TOCSY transfer mechanisms in solids the terms TOBSY (total through-bond correlation spectroscopy) and TOSSY (total through-space correlation spectroscopy) shall be used (*3, 4*). The *J* coupling and the dipolar coupling define, in general, different spin-systems topologies and lead to complementary information. This was, for example, exploited for phosphorus spectroscopy in SiP_2O_7 (*5*), where the use of the *J* coupling partitions the spin system into a sum of two-spin systems (the two ^{31}P spins in a pyrophosphate unit). The use of the dipolar coupling leads to an extended spin system. ^{13}C initial-rate TOSSY and TOBSY experiments on peptides and proteins usually lead to similar spectra because the effective spin systems defined by the two interactions are similar.

Conceptionally, the use of the *J* coupling is simpler and it has the advantage that the polarization transfer is mediated by an isotropic Hamiltonian. Therefore, the transfer is independent of the crystallite orientation. The dipolar interaction, in contrast, is modulated by the MAS rotation and is, to lowest order, averaged to zero. Recoupling experiments have been developed to reintroduce a secular dipolar interaction into the MAS Hamiltonian (e.g., rotational resonance (*6–8*), C7 (*9*), POST-C7 (*10*), CMR7 (*11*), RIL (*12, 13*), DREAM (*14*)). The recoupled dipolar interaction depends on the crystallite orientation.

Despite the advantages mentioned and the fact that the "effective" spin system is smaller and more well-defined in TOBSY experiments, these experiments are not yet widespread. An important reason for this is that TOBSY experiments are technically more demanding than dipolar recoupling because of the relatively small magnitude of the *J* interaction. For a pair of directly bound ^{13}C, it is typically 50 Hz, compared to about 2 kHz for the dipolar coupling. The dipolar interaction and the anisotropic and isotropic chemical-shift differences must be efficiently suppressed for the small *J* couplings to become efficient for polarization transfer. Particular care must be taken to avoid accidental recoupling of anisotropic interactions by the multiple-pulse sequences applied to suppress the isotropic chemical-shift difference terms. In the presence of molecular motion, the TOBSY experiments may be more susceptible to relaxation than TOSSY experiments due to the longer mixing times required. Experiments using the *J* coupling in the context of INADEQUATE experiments have also been described (*15–17*).

The TOBSY experiment of Refs. (*3, 4*) was designed for use with relatively slow MAS frequencies up to about 5 kHz. It employs a mixing sequence of 8 (or 4) modified WALTZ-8 (*18*) composite π pulses per rotor cycle (*3, 4*). The (carbon) RF field strength is 24 times higher than the sample rotation frequency. If only 4 cycles are applied the RF amplitude is lower by a factor of 2, but partial recoupling of the chemical-shift anisotropy occurs.

Often it is desirable to apply considerably higher MAS

[1] Presented, in part, at the 41st ENC, Pacific Grove, CA.

1090-7807/01 $35.00

frequencies, in particular in high magnetic fields. In this contributions we proposed modified TOBSY mixing schemes adapted to MAS frequencies up to 50 kHz. Possible (rotor-synchronized) sequences are identified using lowest order average Hamiltonian theory (*19, 20*). Most sequences considered use supercycles employing the principle of z rotations (*9, 10, 21–23*). The desired lowest order average Hamiltonian consists of the J interaction only:

$$\mathcal{H}_J = \sum_{i<j} 2\pi J_{ij} \mathbf{I}_i \mathbf{I}_j. \qquad [1]$$

The pulse sequences that yield, to zeroth order, the correct Hamiltonian are further characterized by numerical simulations in the framework of the GAMMA simulation environment (*24*). The performance of the best sequence found is confirmed experimentally.

Experiments along the same lines are currently developed by Titman and co-workers (*25*).

2. DESIGN PRINCIPLES

For infinitely fast MAS the relevant Hamiltonian of a ^{13}C spin system approaches the isotropic-phase Hamiltonian that contains the isotropic chemical shifts and the J interaction only. We tacitly assume that proton spins, if present, can be decoupled perfectly. To obtain TOCSY transfer the chemical-shift contribution must be suppressed (*1*). To do so, composite-pulse sequences, e.g., WALTZ-16 (*18*) or DIPSI (*26*), which are broad banded enough to cover the entire spectral range of nuclei like ^{13}C or ^{15}N, are applied.

Practically obtainable MAS frequencies, however, are comparable to the frequencies contained in the multiple-pulse sequence and to the size of the anisotropic interactions which now influence the performance of the pulse sequence. In particular, there is a potential for recoupling of the anisotropic interactions.

An elegant framework to predict the appearance of potential recoupling conditions has been developed by Levitt, Nielsen, and co-workers (*9, 10, 21–23*) using average Hamiltonian theory (*19, 20*). It applies to the particular case of basic pulse sequences using composite pulses with phase ϕ and $\phi + \pi$ and an overall flip angle of an integer multiple of 2π (in Ref. (*23*), sequences using a flip angle of π are also discussed). If N basic multiple-pulse units (denoted as C elements) are applied during n rotor cycles and the phase ϕ of the C elements is incremented in a supercycle by $\nu 2\pi/N$, where ν is an integer which characterizes the pulse sequence, the potential recoupling conditions appear to lowest order as

$$mn - \mu\nu = kN. \qquad [2]$$

m and μ designate the spherical tensor components of the real and spin space parts A_{lm} and $\tilde{T}_{\lambda\mu}$ of the Hamiltonian, respectively, and k is an integer. Such a sequence is denoted by CN_n^ν (*22*). Similar considerations hold for another class of pulse sequences (*23*). For the homonuclear scalar coupling the only nonzero elements are $A_{00} = -\sqrt{3}\, 2\pi J$ and $\tilde{T}_{00} = -(1/\sqrt{3})\mathbf{I}_i\mathbf{I}_j$. The tilde points out that the spin part of the Hamiltonian is—as usual in average Hamiltonian theory—described in an interaction frame with respect to the RF irradiation.

The TOBSY mixing schemes discussed earlier (*3, 4*) can be described using this formalism as $C2_1^0$ and $C4_1^0$ if two WALTZ-8 composite π pulses are combined to form one C element. To denote a specific multiple-pulse unit the general symbol C will be replaced by an abbreviation, in this case $RR2_1^0$ and $RR4_1^0$. As already pointed out in Ref. (*3*) $RR2_1^0$ leads to a recoupling of the CSA interaction (Eq. [2] is fulfilled for $m = 2$, $n = 1$, $\mu = 0, 1$, $\nu = 0$, $N = 2$, and $k = 1$).

For CN_n^ν experiments, the RF amplitude to MAS frequency ratio is given by

$$\omega_1/\omega_r = (N/n)(\tau_C/\tau_1). \qquad [3]$$

τ_C/τ_1 is the ratio of the length of the specific C element to the duration of a 2π pulse. For $RR4_1^0$ Eq. [3] yields a ratio of 24.

For higher MAS frequencies the cycle time of the C element τ_C must be shortened or the ratio N/n must be decreased to avoid high RF power. One is tempted to associate shorter cycle times with inferior offset suppression. However, it must be realized that τ_C refers to the cycle time of a single C element. The z rotations applied in the supercycle will also reject chemical-shift differences, even to higher order, if the C element is properly selected (*10*).

In addition to the RR element mentioned above ($\tau_C/\tau_1 = 6$), and the related sequence $R\bar{R}$ with the same length, we investigated the shorter elements ($90_\phi\ 360_{\phi+\pi}\ 270_\phi$) (the POST element (*10*) which we abbreviate P) and ($360_\phi\ 360_{\phi+\pi}$). Further possibilities, not investigated here, would be two WALTZ-4-R or WALTZ-16-R elements (*18*).

We consider sequences without z rotation supercycles ($\nu = 0$) and with z rotations ($\nu > 0$). Sequences of the first class with overall flip angles $j \cdot 2\pi$, $j > 0$ profit from an effective spin lock. Sequences of the second class exploit the benefit of z rotations to remove unwanted terms from the Hamiltonian according to the spin-space symmetry of the interaction ($\mu = 1, 2$).

For sequences with z rotations and $\nu = 1$ a minimum of $N = 9$ C elements is required to avoid the equality [2]. This leads to $C9_3^1$, $C9_6^1$, $C9_{12}^1$, $C9_{15}^1$, $C9_{21}^1$, $C9_{24}^1$, etc. (all $C9_{p9\pm3}^1$, p integer). Sequences with more RF cycles (e.g., $C10_7^1$, $C10_{13}^1$) or with higher values for ν (e.g., $C9_5^3$, $C15_7^3$) are also possible. For these sequences Eq. [2] can only be fulfilled for $m = \mu = 0$ as desired for selection of the scalar J interaction. The only undesired but symmetry allowed terms are the chemical shift tensors $\tilde{T}_{10}$ with the spatial parts A_{00} or A_{20} and the dipolar term $\tilde{T}_{20}$ with A_{20}. They vanish due to the properties of the C element and MAS, respectively.

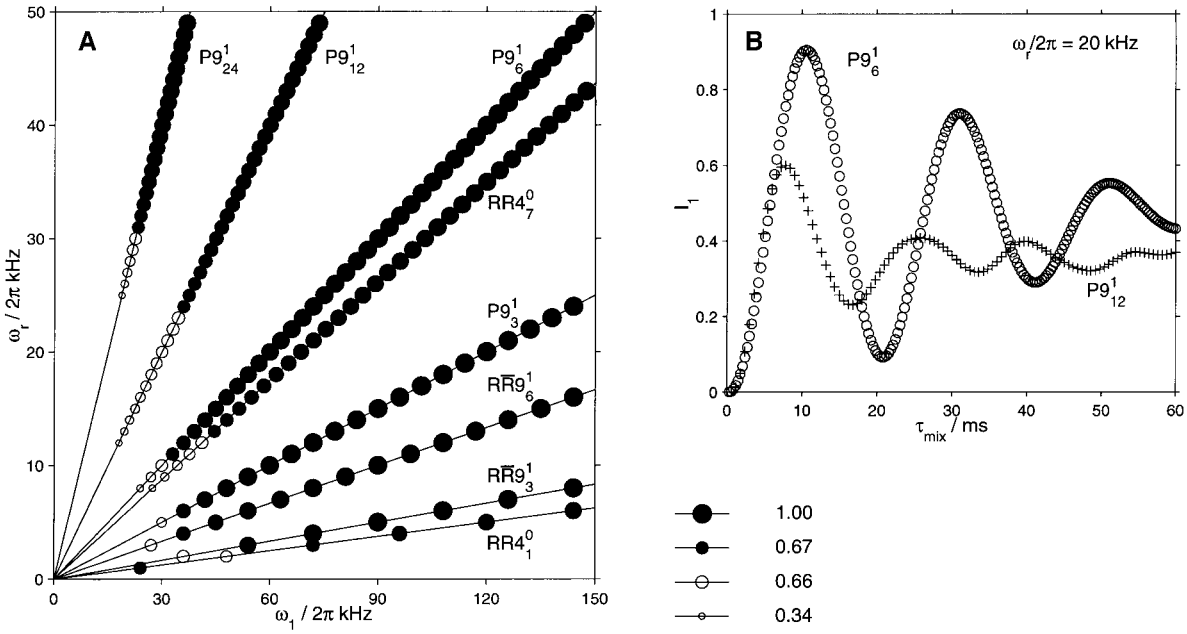

FIG. 1. Simulation of the transfer efficiency for some TOBSY sequences as a function of the RF amplitude and MAS frequency. In A, the diameter of the circles that represents the data points is proportional to the maximum transferred magnetization. Data points that represent a transfer efficiency between 67 and 100% are shown as filled circles, data points between 34 and 66% as open circles, and the ones for less than 33% efficiency are not shown. Two examples of individual transfer curves are shown in B. The model system represents two ^{13}C spins with isotropic chemical shifts of $+6$ and -6 kHz. The dipolar coupling constant was set to 2 kHz, the principal axis being perpendicular to the principal axis chosen for the CSA interactions. For the CSAs anisotropies of 7.5 and 0.5 kHz and asymmetries of 0.1 and 0.05 were used. The scalar coupling constant of 50 Hz is 40 times smaller than the dipolar coupling constant. The propagator for one cycle was calculated in the framework of GAMMA (*24*) using a piecewise constant Hamiltonian. At least 500 time steps per rotor cycle and an average over 200 crystal orientations (*31*) were taken. For sequences using *z* rotations, the simulation started with *z* magnetization on one spin. Sequences without *z* rotations are simulated with initial magnetization on one spin aligned to the direction of the RF field (spin lock).

The sequences listed above can also be used without *z* rotations. However, more sequences exist for $\nu = 0$, e.g., $C3^0_1$, $C4^0_1$, $C3^0_7$, $C4^0_7$, $C4^0_9$, $C5^0_9$, $C6^0_8$, $C7^0_9$. All of these sequences avoid the fulfillment of Eq. [2] except for $m = 0$. Again, the remaining symmetry-allowed terms, except for the *J* coupling, are averaged by magic-angle spinning and by the spin-space rotations of the C element.

All of the sequences mentioned lead, in zeroth-order average Hamiltonian theory, to the same Hamiltonian (pure *J* coupling).

3. NUMERICAL SIMULATIONS

The Hamiltonian for all sequences discussed is equal in lowest order, but the exact Hamiltonian will be different due to terms not taken into account in lowest order. To assess their magnitude for typical parameters of a ^{13}C or ^{15}N spin system, we have performed numerical simulations in the framework of GAMMA (*24*). As a model, a coupled two-spin system with all interactions mentioned was used. Figure 1A shows a simulation of the transfer efficiency as a function of RF amplitude and MAS frequency. Each sequence is characterized by a straight line. The transfer efficiency is encoded in the size of the marker. Spin-system parameters used are given in the figure legend. The value of the first (and usually highest) maximum of the individual buildup curves (see the two examples in Fig. 1B) is shown. For all sequences which give a transfer of more than 50% the polarization-transfer curves show a damped oscillatory behavior (similar to Fig. 1B) with a frequency close to the *J* coupling constant. Pulse sequences with "poor" performance are omitted from Fig. 1A, e.g., all sequences with the simple $(360_\phi\ 360_{\phi+\pi})$ C element.

Most sequences with good performance use *z* rotations in the supercycle. Exceptions are the "original" $RR4^0_1$ TOBSY as well as $RR4^0_7$. The shortest supercycle, $RR3^0_1$, gave only poor results.

All the other sequences with high transfer efficiency represented in Fig. 1A employ *z* rotations, showing the benefit of this technique for TOBSY mixing sequences. For "slow" MAS $R\bar{R}9^1_3$ and $R\bar{R}9^1_6$ with the $R\bar{R}$ unit perform well. For higher MAS frequencies the sequences $P9^1_3$, $P9^1_6$, $P9^1_{12}$, and $P9^1_{24}$ show a good transfer (in contrast to $P9^1_{15}$ and $P9^1_{21}$).

The best pulse sequence for the MAS frequency range from about 12 kHz to about 30 kHz is $P9^1_6$. For even higher spinning frequencies $P9^1_{12}$ and $P9^1_{24}$ become more favorable.

To further characterize the influence of isotropic shift differences on $P9^1_6$ at 20 kHz MAS one spin is set on-resonance while the offset of the other spin is varied. A transfer efficiency of more than 90% is obtained for offsets up to 11 kHz. This is considerably better than for $RR4^0_1$ at 5 kHz MAS, where the

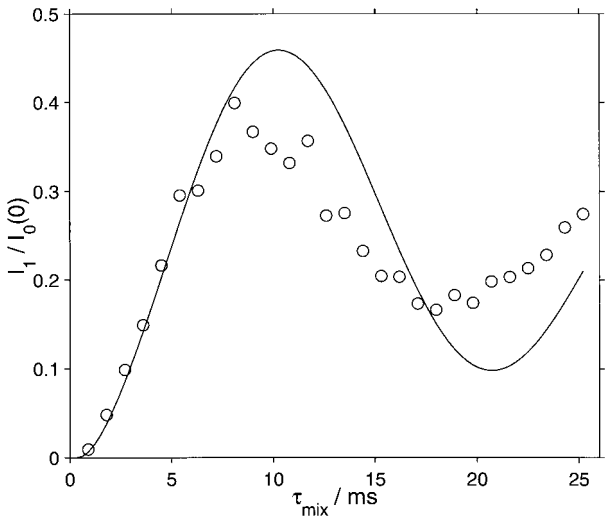

FIG. 2. Experimental buildup curve obtained for a fully ^{13}C-labeled zinc acetate powder using the TOBSY-P9$_6^1$ sequence at a MAS frequency of 20 kHz. All measurements were performed on a Chemagnetics CMX Infinity 300 spectrometer equipped with a 2.5-mm double-resonance probe. A *z* filter (*32*) is used to prepare initial *z* polarization on the carboxyl carbon ($I_0(\tau_{mix} = 0)$). An RF amplitude of 135 kHz was used for Lee–Goldburg (*27*) decoupling during the mixing time. The amplitude, pulse duration, and angle for TPPM (*33*) decoupling during the acquisition were 126 kHz, 3.7 μs, and 18°, respectively. The polarization transferred to the methyl carbon (I_1) is obtained by integration of the methyl peak as a function of the mixing time. The RF carrier frequency is centered between the two resonance frequencies. The result of a simulation using an inhomogeneous RF field is shown as a solid line. The field strength probability was assumed to be constant between −14 and +1% of the nominal value.

transfer efficiency drops dramatically for offsets higher than 5 kHz, although the RF amplitude in the latter is twice as high.

So far, we have not considered the influence of RF inhomogeneities. For P9$_6^1$ at 20 kHz MAS a transfer efficiency of more than 90% is observed for deviations of 3% from the nominal RF amplitude. It drops below 60% for deviations of 5%, indicating that the RF inhomogeneity limits the transfer efficiency in practical cases.

Furthermore, we have simulated the TOBSY mixing sequences suggested in Ref. (*23*). A simple or composite π pulse was used in order to obtain an RF amplitude to MAS frequency ratio of 3 or close to 3. These sequences are somewhat less sensitive to deviations of the RF amplitude from the nominal value. The transfer efficiency in the simulations is, however, significantly lower than for the sequences shown in Fig. 1A. Another sequence that was tested in simulation and experiment is P12$_8^3$. It uses only $\pi/2$ phase increments, which is advantageous for some older spectrometers. The performance, however, is considerably lower than that of P9$_6^1$ (at the same RF amplitude to MAS frequency ratio).

While the ideal *J*-coupling Hamiltonian is isotropic in spatial and spin coordinates, the error terms will, in general, be anisotropic. In our simulations we have observed that sequences using *z* rotations perform best (in the sense of the results plotted in Fig. 1A) with *z* magnetization as initial condition. RR sequences without *z* rotations perform best under spin-lock conditions. P sequences have been found to benefit significantly from *z* rotations. In the presence of *z* rotations, R$\bar{\text{R}}$ sequences seem preferred over the RR sequences.

The simulations presented did not take into account the influence of the protons (and other heterospins). We have assumed that those are perfectly decoupled. In fact, this assumption is not fully warranted. The remaining proton couplings can lead to spin-diffusion cross peaks and $T_{1\rho}$ relaxation which deteriorates the signal-to-noise ratio (TOBSY requires relatively long mixing times). To facilitate decoupling, either by on-resonance or Lee–Goldburg (*3, 27*) irradiation on the protons, it is beneficial to keep the (carbon) RF low because a ratio of about 3 or higher between carbon and decoupling field is, as a rule of thumb, required for efficient decoupling (*28, 29*).

4. EXPERIMENTS

An experimental polarization-transfer curve obtained for fully ^{13}C-labeled zinc acetate using P9$_6^1$ at a MAS frequency of 20 kHz is given in Fig. 2. The pulse sequence is depicted in Fig. 3. A damped oscillatory transfer with a maximum of 40% after about 9 ms is observed. This is strong evidence that the transfer is indeed mediated by the *J* coupling. Given the

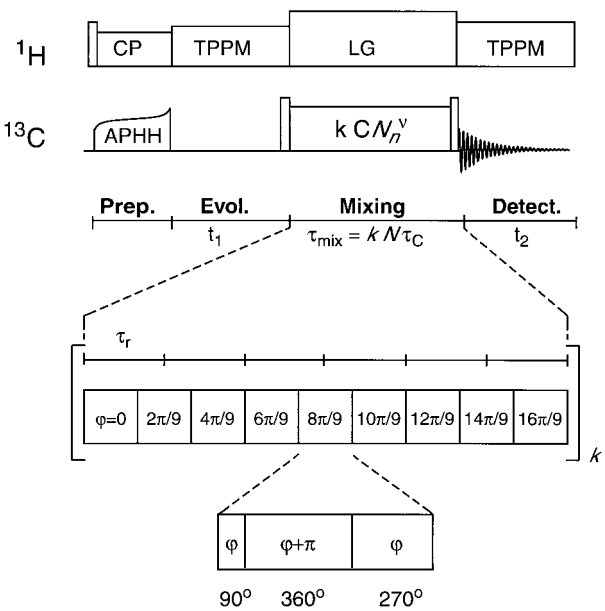

FIG. 3. Pulse scheme for TOBSY with the P9$_6^1$ mixing sequence. Transverse carbon magnetization is created by APHH-CP (*34*). During the evolution and detection periods TPPM (*33*) proton decoupling is used. Undesired transverse components are removed by adding signals with initial plus and minus *z* magnetization in the phase cycle. Lee–Goldburg (*27*) homonuclear proton decoupling is applied in the mixing sequence. For the measurement of the polarization-transfer curve by 1D experiments the evolution time is set to one-quarter of the inverse chemical-shift difference and an additional delay of 10 ms without RF irradiation is added after the first ^{13}C $\pi/2$ pulses (*32*).

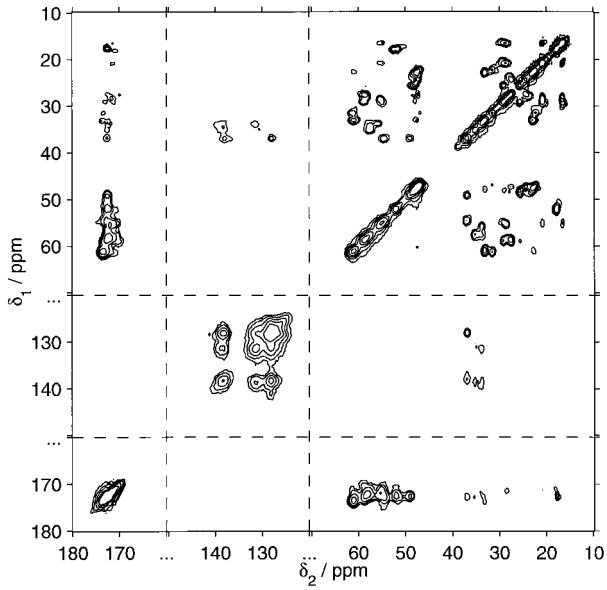

FIG. 4. TOBSY with the $P9_6^1$ mixing sequence of a uniformly ^{13}C-labeled antamanide powder sample using a mixing time of 7.2 ms. The spinning frequency was set to 20 kHz and the carbon RF amplitude to 60 kHz. Decoupling parameters are given in the legend to Fig. 2. The data set consists of 1024 complex data points in t_2 and 256 complex data points in t_1. Sixteen scans per increment were accumulated using the States scheme. Gaussian broadenings of 16 and 32 Hz were applied in t_2 and t_1, respectively. Five contour levels between 1 and 16% of the maximum peak hight with a multiplier of 2 are plotted. The spectral regions between 70–120 and 150–160 ppm contain no peaks and are omitted from the plot.

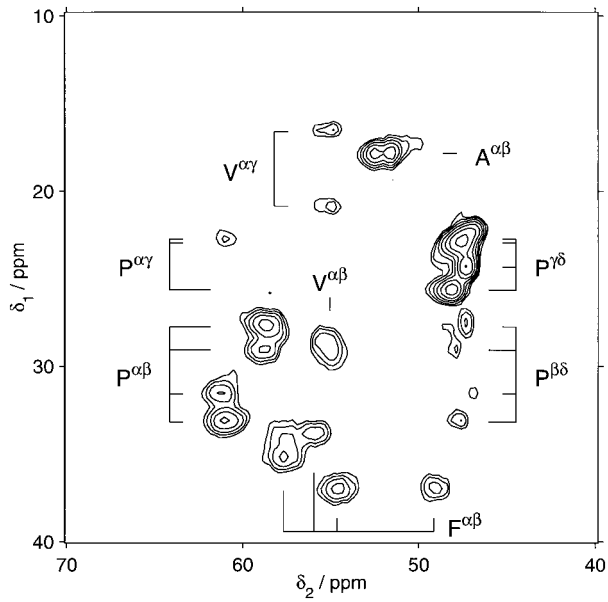

FIG. 5. Expansion of a cross peak region from Fig. 4 with the intraresidue assignment (A = Ala, P = Pro, V = Val, F = Phe). Seven contour levels between 1 and 11% of the maximum intensity in the entire spectrum using a multiplier of 1.5 are displayed.

coupling constant of 52 Hz (from a dissolved sample), the theoretical maximum occurs after 9.6 ms. The integrals are normalized to the initial sum polarization. The decay of the sum polarization (not shown) is about 10% after 10-ms mixing time, indicating that the proton decoupling is rather efficient under our experimental conditions. The experiments were performed using a completely filled rotor (no sample restriction). Also shown in Fig. 2 is a simulation using an inhomogeneous RF field. The RF amplitude probability was assumed to be constant between -14 and $+1$% of the nominal value and zero outside this range. The good agreement between the oversimplified model and the experiment is probably fortuitous.

The TOBSY spectrum of a uniformly ^{13}C-labeled powder sample of the cyclic decapeptide antamanide (Val^1–Pro^2–Pro^3–Ala^4–Phe^5–Phe^6–Pro^7–Pro^8–Phe^9–Phe^{10}) using the $P9_6^1$ mixing sequence is shown in Fig. 4 for 20 kHz MAS and a mixing time of 7.2 ms.

The signal loss due to relaxation (by molecular motion) and pulse imperfections has been evaluated by comparing the integrated signal intensities to the ones in an experiment with no TOBSY mixing period. For the C′ and C^α resonances, the signal loss is less than 20%. For the aromatic carbons, it lies between 30 and 40%.

An expansion of the cross-peak region between the two low-frequency groups is shown in Fig. 5. Strong cross peaks are observed for all 14 one-bond couplings, namely the C^α–C^β peaks of all 10 amino acids and the 4 proline C^γ–C^δ cross peaks. Also visible are the C^β–C^δ and 1 C^α–C^γ proline two-bond cross peaks. The proline C^β–C^δ cross peaks can be used to resolve the signals from the only two spin systems (of the 14) that show strong overlap for the one-bond cross peaks. Also visible are the 2 valine C^α–$C^{\gamma 1}$ and C^α–$C^{\gamma 2}$ two-bond cross peaks. For the alanine C^α–C^β cross peak, two signals separated by about 80 Hz in the ω_2 dimension are observed. This is probably due to the presence of two antamanide conformations in the sample. In Table 1, the mean of the two

TABLE 1
Assignment of the ^{13}C Resonances in Antamanide to the Amino Acids

	Chemical shift/ppm				
AA	C′	C^α	C^β	C^γ	C^δ
Val	171.4	54.9	28.7	16.6/20.9[a]	
Ala	171.7[b]	52.0[b]	17.9		
Pro_I	173.1	58.8	29.2	25.6	47.9
Pro_{II}	173.4	61.2	31.5	22.3	46.8
Pro_{III}	172.4	58.7	27.5	24.4	47.3
Pro_{IV}	173.7	61.0	33.1	22.9	47.6
Phe_I	172.3	55.9	33.8	[c]	[c]
Phe_{II}	172.7	49.0	37.0	[c]	[c]
Phe_{III}	172.7	54.5	37.0	[c]	[c]
Phe_{IV}	172.6	57.7	35.2	[c]	[c]

[a] Valine has two C^γ.
[b] Mean of two shifts; see text.
[c] Not assigned.

maxima in the ω_2 dimension (52.4 and 51.6 ppm) is given for C^{α}. A similar observation is made for the alanine C'–C^{β} cross peaks. The value for C' given in Table 1 is again a mean of two maxima in the ω_2 dimension (172.5 and 170.9 ppm).

In the frequency range between 0 and 30 ppm, seven pairs of cross peaks are found: the two valine C^{β}–$C^{\gamma 1}$ and C^{β}–$C^{\gamma 2}$ (one-bond), the valine $C^{\gamma 1}$–$C^{\gamma 2}$ (two-bond), and the four proline C^{β}–C^{γ} (one-bond). The two prolines with a small chemical-shift difference between C^{β} and C^{γ} have been assigned to prolines with a trans peptide-bond configuration (Pro^2 and Pro^7) (*30*) and the ones with a larger separation to cis prolines (Pro^3 and Pro^8).

For an experiment with a mixing time of 3.6 ms, the two-bond cross peaks of proline C^{β}–C^{δ}, valine C^{α}–C^{γ}, and the weak proline C^{α}–C^{γ} cross peaks disappear. For 14.4-ms mixing time, they are more pronounced.

The TOBSY cross peaks observed are sufficient to assign all carbon signals, except the aromatics, to the respective spin systems. The assignment deduced from the TOBSY data is listed in Table 1. It should be noted that some of the chemical shifts observed deviate (up to 2.7 ppm) from the values given in Ref. (*30*). We have found that the chemical shifts depend strongly on the preparation of the sample, in particular on the water content.

5. CONCLUSIONS

Pulse sequences for total through-bond correlation spectroscopy at MAS frequencies up to 50 kHz have been found. An application to a decapeptide at 20 kHz MAS was demonstrated. The spin systems of all 10 amino acids can be identified from the TOBSY spectrum. The decay of the sum polarization ("effective $T_{1\rho}$ relaxation") is so slow that the relatively long mixing times for transfer via the scalar coupling can be realized without significant loss in the signal-to-noise ratio. In the absence of large scale molecular motions, the TOBSY schemes discussed should therefore also be applicable to larger peptides or to proteins.

ACKNOWLEDGMENTS

We thank Dr. Andreas Detken for scientific advice. Financial support by the Swiss National Science Foundation is acknowledged. One of the authors, E.H.H., thanks the Deutsche Forschungsgemeinschaft for a grant.

REFERENCES

1. L. Braunschweiler and R. R. Ernst, *J. Magn. Reson.* **53,** 521–528 (1983).
2. R. R. Ernst, G. Bodenhausen, and A. Wokaun, "Principles of Nuclear Magnetic Resonance in One and Two Dimensions," Clarendon Press, Oxford, 1987.
3. M. Baldus and B. H. Meier, *J. Magn. Reson. A* **121,** 65–69 (1996).
4. M. Baldus, R. J. Iuliucci, and B. H. Meier, *J. Am. Chem. Soc.* **119,** 1121–1124 (1997).
5. R. J. Iuliucci and B. H. Meier, *J. Am. Chem. Soc.* **120,** 9059–9062 (1998).
6. M. G. Colombo, B. H. Meier, and R. R. Ernst, *Chem. Phys. Lett.* **146,** 189–196 (1988).
7. D. P. Raleigh, M. H. Levitt, and R. G. Griffin, *Chem. Phys. Lett.* **146,** 71–76 (1988).
8. M. H. Levitt, D. P. Raleigh, F. Creuzet, and R. G. Griffin, *J. Chem. Phys.* **92,** 6347–6364 (1990).
9. Y. K. Lee, N. D. Kurur, M. Helmle, O. G. Johannessen, N. C. Nielsen, and M. H. Levitt, *Chem. Phys. Lett.* **242,** 304–309 (1995).
10. M. Hohwy, H. J. Jakobsen, M. Edén, M. H. Levitt, and N. C. Nielsen, *J. Chem. Phys.* **108,** 2686–2694 (1998).
11. C. M. Rienstra, M. E. Hatcher, L. J. Mueller, B. Sun, S. W. Fesik, and R. G. Griffin, *J. Am. Chem. Soc.* **120,** 10602–10612 (1974).
12. M. Baldus and B. H. Meier, *J. Magn. Reson.* **128,** 172–193 (1997).
13. M. Baldus, M. Tomaselli, B. H. Meier, and R. R. Ernst, *Chem. Phys. Lett.* **230,** 329–336 (1994).
14. R. Verel, M. Baldus, M. Ernst, and B. H. Meier, *Chem. Phys. Lett.* **287,** 421–428 (1998).
15. A. Lesage, C. Auger, S. Calderelli, and L. Emsley, *J. Am. Chem. Soc.* **119,** 7867–7868 (1997).
16. A. Lesage, M. Bardet, and L. Emsley, *J. Am. Chem. Soc.* **121,** 10987–10993 (1999).
17. R. Verel, J. D. van Beek, and B. H. Meier, *J. Magn. Reson.* **140,** 300–303 (1999).
18. A. J. Shaka, J. Keeler, and R. Freeman, *J. Magn. Reson.* **53,** 313–340 (1983).
19. U. Haeberlen and J. S. Waugh, *Phys. Rev.* **175,** 453–467 (1968).
20. U. Haeberlen, High resolution NMR in solids, *Adv. Magn. Reson.* **Suppl. 1** (1976).
21. M. Hohwy, C. M. Rienstra, C. P. Jaroniec, and R. G. Griffin, *J. Chem. Phys.* **110,** 7983–7991 (1999).
22. M. Edén and M. H. Levitt, *J. Chem. Phys.* **111,** 1511–1519 (1999).
23. M. Carravetta, M. Edén, X. Zhao, A. Brinkmann, and M. H. Levitt, *Chem. Phys. Lett.* **321,** 205–215 (2000).
24. S. Smith, T. Levante, B. H. Meier, and R. R. Ernst, *J. Magn. Reson. A* **106,** 75–105 (1994).
25. A. Heindrichs, H. Geen, and J. Titman, "Through Bond Correlation Spectroscopy in Solids," Poster presented at the 41st ENC, 2000.
26. A. J. Shaka, C. J. Lee, and A. Pines, *J. Magn. Reson.* **77,** 274–293 (1988).
27. M. Lee and W. I. Goldburg, *Phys. Rev.* **140,** A1261–1271 (1965).
28. Y. Ishii, J. Ashida, and T. Terao, *Chem. Phys. Lett.* **246,** 439–445 (1995).
29. A. E. Bennett, C. M. Rienstra, J. M. Griffiths, W. Zhen, P. T. Lansbury, Jr., and R. G. Griffin, *J. Chem. Phys.* **108,** 9463–9479 (1998).
30. S. K. Straus, T. Bremi, and R. R. Ernst, *J. Biomol. NMR* **10,** 119–128 (1997).
31. V. B. Cheng, H. H. Suzukawa, and M. Wolfsberg, *J. Chem. Phys.* **59,** 3992–3999 (1973).
32. O. W. Sørensen, M. Rance, and R. R. Ernst, *J. Magn. Reson.* **56,** 527–534 (1984).
33. A. E. Bennett, C. M. Rienstra, M. Auger, K. V. Lakshmi, and R. G. Griffin, *J. Chem. Phys.* **103,** 6951–6958 (1995).
34. S. Hediger, B. H. Meier, and R. R. Ernst, *Chem. Phys. Lett.* **240,** 449–456 (1995).